Published in final edited form as:
Life Sci. 2022 November 01; 308: 120916. doi:10.1016/j.lfs.2022.120916.

Modulation of cardiac voltage-activated K^+ currents by glypican 1 heparan sulfate proteoglycan

Diego Santos Souza[1], **Andreia Zago Chignalia**[1,2,3], **Joao Luis Carvalho-de-Souza**[*,1,2,4,5]

[1]Department of Anesthesiology, College of Medicine, University of Arizona, Tucson, AZ 85724 USA.

[2]Department of Physiology, College of Medicine University of Arizona, Tucson, AZ 85724 USA.

[3]Department of Pharmacology and Toxicology, College of Pharmacy, University of Arizona, Tucson, AZ 85724.

[4]Department of Ophthalmology and Visual Sciences, College of Medicine, University of Arizona, Tucson, AZ 85724.

[5]BIO5 Institute, University of Arizona, Tucson, AZ 85724

Abstract

Background: Glypican 1 (Gpc1) is a heparan sulfate proteoglycan attached to the cell membrane via a glycosylphosphatidylinositol anchor, where it holds glycosaminoglycans nearby. We have recently shown that Gpc1 knockout (*Gpc1*$^{-/-}$) mice feature decreased systemic blood pressure. To date, none has been reported regarding the role of Gpc1 on the electrical properties of the heart and specifically, in regard to a functional interaction between Gpc1 and voltage-gated K^+ channels.

Methods: We used echocardiography and *in vivo* (electrocardiographic recordings) and *in vitro* (patch clamping) electrophysiology to study mechanical and electric properties of mice harts. We used RT-PCR to probe K^+ channels' gene transcription in heart tissue.

Results: *Gpc1*$^{-/-}$ hearts featured increased cardiac stroke volume and preserved ejection fraction. *Gpc1*$^{-/-}$ electrocardiograms showed longer QT intervals, abnormalities in the ST segment, and delayed T waves, corroborated by longer action potentials in isolated ventricular cardiomyocytes. In voltage-clamp, these cells showed decreased I_{to} and I_K voltage-activated K^+ current densities. Moreover, I_K showed activation at less negative voltages, but a higher level of inactivation at a given membrane potential. Kcnh2 and Kcnq1 voltage-gated K^+ channels subunits' transcripts were remarkably more abundant in heart tissues from *Gpc1*$^{-/-}$ mice, suggesting that Gpc1 may interfere in the steps between transcription and translation in these cases.

[*]Corresponding author: Joao L. Carvalho-de-Souza. jcds@anesth.arizona.edu.

Author Contribution

JCdS and AZC conceived the study. DSS performed research and analyzed the data with guidance from JCdS. DSS and JCdS wrote the paper and received important inputs from AZC.

Disclosures

None.

Conclusion: Our data reveals an unprecedented connection between Gpc1 and voltage-gated K^+ channels expressed in the heart and this knowledge contributes to the understanding of the role of this HSPG in cardiac function which may play a role in the development of cardiovascular disease.

Graphical Abstract

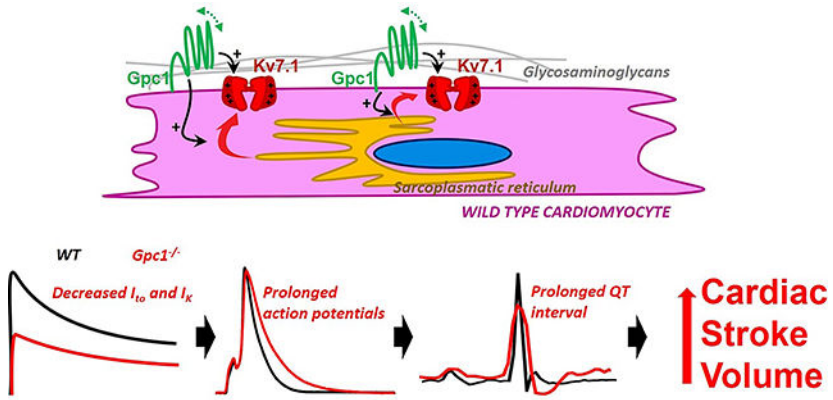

Keywords

Glypican 1; voltage-activated K^+ currents; transient outward current; delayed rectifiers; hypertension

Introduction

Glypican 1 (Gpc1) has emerged as an important modulator of cardiovascular function. We have recently shown that Gpc1 global knockout mice (*Gpc1*$^{-/-}$) present with cardiac left ventricular hypertrophy without changes in collagen deposition suggestive of a proliferative phenotype in ventricular cardiomyocytes [1]. In addition, we also found *Gpc1*$^{-/-}$ mice exhibiting lower systolic blood pressure and unable to develop hypertension after chronic treatment with norepinephrine. In this last study we found the vascular noradrenergic response in *Gpc1*$^{-/-}$ mice to be impaired by disrupted intracellular calcium handling and we were able to pinpoint decreased IP3 receptor activity as a crucial player in Gpc1-mediated noradrenergic signaling [2]. To date, the effects of Gpc1 on heart function and specifically on cardiac electrophysiology are unknown.

In humans, glypican is a six-member family (Gpc1–6) of heparan sulfate proteoglycans (HSPG) that are bound to the plasma membrane by a glycosylphosphatidylinositol (GPI) anchor. Glypicans are essentially extracellular proteins that specifically carry heparan sulfate glycosaminoglycans (GAG) on their extracellular domain, covalently attached to the core protein that is thought to be critical for functional interactions with surface receptors [3], [4]. It has been described that the core protein of HSPG can have independent function. Nevertheless, the abundance of attached GAG determines the ligand-biding capacity of the HSPG and thus, has a key role in determining the core protein biological function [5].

The role of Gpc1 on ion channels functionalities is virtually unexplored. It was recently shown that the enzymatic digestion of GAG from endothelial cells affect flow-induced

dilation mediated by inwardly rectifying K^+ channels (K_{ir}) in endothelial cells isolated from mesenteric adipose arteries of obese mice[6]. In addition, the glycocalyx thickness was associated with the functionality of the same K_{ir} channels in visceral adipose arteries and subcutaneous adipose arteries from obese mice and humans[7]. Voltage-gated proton channels were recently reported to be modulated by HSPG [8]. Remarkably, to date, there are no reports in the literature aiming at studying the functional connection between glypicans and voltage-gated K^+ channels (VGKC).

In this present paper we show original data from studies of various electrophysiological aspects of global Gpc1 knockout (*Gpc1*$^{-/-}$) mice hearts, seeking alterations that would be in the context of our recent histological and functional cardiovascular findings in these animals. First, we show by electrocardiography increased cardiac stroke volume and cardiac output with preserved ejection fraction in *Gpc1*$^{-/-}$ mice. Second, surface electrocardiographic recordings additionally demonstrated longer QT intervals, abnormalities in the ST segment, and delayed T waves, proposing *Gpc1*$^{-/-}$ hearts may pump blood with extended systoles. Next, at the cellular level, in isolated ventricular cardiomyocytes, we show longer action potentials and a stunning 50% overall depression on the density of voltage-activated K^+ currents in addition to biophysical alterations such as in the channels' voltage dependence processes.

Altogether, our data indicate that Gpc1 is crucial for cardiac electrophysiology since it strongly modulates the abundancy and the biophysical properties of voltage-activated K^+ currents in the cardiac tissue. This modulation would have critical consequences for the cardiac physiology as a pump. Our data contributes with new knowledge for studies aiming at targeting the cardiac dynamics with newly developed therapeutics interventions. We present Gpc1 as a potential player for the development of new therapeutic agents, which may be particularly important in pro-arrhythmic cardiac diseases.

Results

To assess the role of glypican 1 in heart electrophysiology we have used *Gpc1*$^{-/-}$ mice that was developed in a CD1 genetic background. CD1 mice (wild type) served as control in all experiments (see methods section for details).

Gpc1$^{-/-}$ mice feature altered cardiac cycle dynamics.

The cardiac function of *Gpc1*$^{-/-}$ mice was assessed by transthoracic echocardiography (Echo). Echo analysis showed no statistical difference in end-systolic and end-diastolic volumes, and in the ejection fraction between *Gpc1*$^{-/-}$ and CD1 mice data. However, *Gpc1*$^{-/-}$ mice showed increased stroke volume and therefore increased cardiac output when compared to CD1 mice (Table 1), suggesting prolonged systolic phase in *Gpc1*$^{-/-}$ mice.

Electrocardiographic waves show abnormal S-T segment in *Gpc1*$^{-/-}$ mice.

Abnormalities in myocardial electric signals are commonly associated with changes in cardiac mechanical function such as stroke volume and cardiac output, found here by Echo analysis in *Gpc1*$^{-/-}$ mice (Table 1). To assess whole heart electrical properties, electrocardiograms (ECG) using lead II, aiming at a ventricular signal, were performed

on anesthetized mice (Fig. 1). Compared to data from CD1 mice, electrocardiographic waves from *Gpc1*$^{-/-}$ mice presented significantly prolonged QT intervals, a high frequency of abnormal S-T segments, and prolonged T waves (Table 2). Abnormal S-T segments were characterized by deviations of the recorded segment relative to the isoelectric line denoting suggesting abnormal ventricular repolarization.

Action potentials from *Gpc1*$^{-/-}$ ventricular cardiomyocytes show delayed repolarization phase

The significant alterations in S-T segments and T waves in ECG from *Gpc1*$^{-/-}$ mice strongly indicate delayed ventricular cardiomyocytes repolarization after an action potential is fired. The S-T segments in electrocardiography are timely related to the systole period and the T wave itself represents the ventricular repolarization that determines the diastole onset.

We recorded action potentials in isolated ventricular cardiomyocytes and the results explicitly confirm the anticipated notion of longer action potentials in ventricular cardiomyocytes from *Gpc1*$^{-/-}$ mice as compared with CD1-cardiomyocytes. The repolarization periods are consistently longer in *Gpc1*$^{-/-}$ mice ventricular cardiomyocytes (Fig. 2). Detailed analysis revealed no statistical differences in the ventricular cardiomyocytes' parameters affecting excitability such as resting potential, action potentials peak-to-peak amplitude, peak value, maximal rise slope, or the maximal decay slope (Table 3).

Gpc1$^{-/-}$ ventricular cardiomyocytes show reduced voltage activated K^+ currents featuring changed voltage dependences.

Families of voltage-activated K^+ currents recorded under voltage-clamp on ventricular cardiomyocytes from *Gpc1*$^{-/-}$ and CD1 mice are showed as typical traces in Fig 3A and 3B. From each current trace, a sample of I_{to} currents is taken from the currents' peak, and a sample of I_K is taken at the end of the traces, after 300 ms of depolarization. The amplitude of both I_{to} and I_K currents densities throughout the current-voltage (I-V) curves are significantly reduced in *Gpc1*$^{-/-}$ ventricular cardiomyocytes relative to CD1 data to 47% and 51% of the currents' levels, respectively (Figs 3C and 3D). Individual I-V curves were transformed into conductance-voltage (G-V) curves by using Ohm's law, normalized and averaged, yielding the data showed in Figs 3E and 3F. Individual G-V curves (from I_{to} and I_K) were normalized by their maxima and fitted with Boltzmann's formalism to yield, for each individual cell studied, a $V_{1/2}$, the voltage related to activation of 50% of maximal conductance, and the maximum slope that relates to voltage sensitivity of the currents. Individual $V_{1/2}$ values from I_{to} and I_K, respectively, are plotted on Figs 3G and 3H. As the data show, the voltage-dependence of I_K, but not I_{to}, is indeed changed in *Gpc1*$^{-/-}$ as compared to data from CD1 ventricular cardiomyocytes: $V_{1/2}$ for I_{to} is −16.22±1.81 mV for CD1 and −11.05±1.99 mV for *Gpc1*$^{-/-}$ ventricular cardiomyocytes, whereas 50% of I_K is activated at −3.55±2.61 mV in CD1 and at 15.08±3.69 mV in *Gpc1*$^{-/-}$ ventricular cardiomyocytes. Averaged $V_{1/2}$ and the maximum slope derived from fittings are shown in Table 4.

Changes in inactivation processes of the K^+ currents may contribute to delayed repolarization in ventricular cardiomyocytes from *Gpc1*$^{-/-}$ mice.

Next, we investigated the inactivation process of the K^+ currents in the ventricular cardiomyocytes from CD1 and *Gpc1*$^{-/-}$ mice. The inactivation kinetics during a depolarized periods showed no difference between the ventricular cardiomyocytes from CD1 and *Gpc1*$^{-/-}$ mice (Supplementary Fig 1).

We also evaluated the steady-state voltage dependent inactivation of both I_{to} and I_K. We studied the amplitude of I_{to} and I_K at several membrane potentials at +60 mV after a 300 ms pre-pulse at several voltages, one at a time. This conditioning pulse duration is 10-fold longer than the action potentials in mice ventricular cardiomyocytes and therefore it covers the physiological significance of voltage-dependent inactivation. Typical currents recorded with the above voltage clamp protocol is shown in Fig. 4A and 4B. I_{to} (peak) and I_K (end of a 300 ms depolarization to +60 mV) were normalized by their respective maxima that was after a −100 mV conditioning period in most cases. The amplitude of the currents activated (available current) during the +60 mV were averaged and plotted against the respective conditioning voltage (Figs 4C and 4E). The voltage-dependent inactivation of I_{to} seems to be only slightly, non-significantly affected in *Gpc1*$^{-/-}$ ventricular cardiomyocytes. However, I_K currents in *Gpc1*$^{-/-}$ ventricular cardiomyocytes inactivate at a much more negative voltages as compared to currents from CD1 mice. Whole inactivation curves from individual cells were fitted with the Boltzmann's formalism. $V_{1/2}$, the voltage related to the inactivation of 50% of the currents during the conditioning pulse were plotted and showed in Fig. 4D and 4F for I_{to} and I_K, respectively. As expected by the average inactivation curves' shapes, I_K, but not I_{to} from *Gpc1*$^{-/-}$ ventricular cardiomyocytes present significantly different $V_{1/2}$ values when compared to data from CD1 ventricular cardiomyocytes. The voltage that inactivates 50% of I_{to} is −49.38±1.72 mV for CD1 and −54.72±5.90 mV for *Gpc1*$^{-/-}$ ventricular cardiomyocytes, whereas 50% of I_K is inactivated by −29.19±1.66 mV in CD1 and −46.84±6.78 mV in *Gpc1*$^{-/-}$ ventricular cardiomyocytes. All fitting-derived parameters from inactivation analysis is shown in Table 5.

The recovery from inactivation in I_{to} and I_K are both altered in *Gpc1*$^{-/-}$ mice.

At resting potential, K^+ channels must recover from inactivation process in order to be activated once again by membrane depolarization. We studied the recovery from a full inactivating event, established by a 300 ms depolarization period at +60 mV, using voltage clamp, by means of using the classic three pulses protocol to probe the recovering. The first pulse to +60 mV lasts 300 ms and is intended to fully inactivate I_{to} and I_K. The second pulse, time-varying and at holding potential, is intended to recover the currents from inactivation in a voltage- and time-dependent process. Finally, the third pulse to +60 mV is intended to activate the currents recovered from inactivation during the second pulse. Therefore, the recovery from inactivation is expressed as the ratio between the currents during the third pulse relative to currents in the first pulse. Typical currents recorded with this voltage protocol are shown (Fig. 5A and 5B). Averaged recovery from inactivation data for I_{to} and I_K were plotted against the time recovery (the duration of the second pulse) (Fig. 5C and 5F). Each full set of recovery from inactivation data (from each individual cell studied, from CD1 and *Gpc1*$^{-/-}$ ventricular cardiomyocytes) was individually fitted by a

single exponential to generate a time constant and a linear factor that is the non-inactivated fraction of the currents. Data show that the time recovery from inactivation of I_{to}, but not I_K, was significantly delayed in *Gpc1*$^{-/-}$ cells compared to CD1 ventricular cardiomyocytes. In contrast, the non-inactivated fraction of the currents, or the currents recovered in less than 10 ms (the shortest second pulse duration) was not altered for I_{to} currents from *Gpc1*$^{-/-}$, but significantly decreased for I_K in *Gpc1*$^{-/-}$ ventricular cardiomyocytes (Fig. 5E and 5H). All fitting parameters are shown in Table 6.

K^+ ion channels mRNA expression in *Gpc1*$^{-/-}$ mice.

Finally, we surveyed the abundance of mRNA for many cardiac K^+ ion channels' subunits in *Gpc1*$^{-/-}$ mice ventricular cardiac tissue as means of detecting possible alterations in gene expression that would match the functional data shown here. We used reverse transcriptase cDNA synthesis from mRNA templates extracted and purified from cardiac ventricular tissues, from CD1 and *Gpc1*$^{-/-}$ mice. Next, we amplified gene targets by real time quantitative polymerase chain reactions (rt-qPCR). Our exhaustive list of target genes was based on many previously reported studies of murine ventricular cardiomyocytes ion channels expression [9]–[13]. The ssDNA oligos used as primers in this study are shown in Supplementary Table 1. The target genes were split in three categories: genes encoding protein subunits channels related to I_{K1} (*Kcnj2, Kcnj3, Kcnj5, Kcnj8, Kcnj11, Kcnj12*), to I_{to} (*Kcna7, Kcnd2* and *Kcnd3*), and to I_K (*Kcna5*, *Kcnb1*, *Kcnh2*, *Kcnq1*, *Kcne1*, *Kcnv2* and *Kcng2*). It is noteworthy to mention the presence of *Kcng2* and *Kcnv2* in many studies. The product of these two genes do not form conductive homotetrameric channels, the reason why they were named silent. The rationale of these genes in our list will be further explained in the discussion section. Our rt-qPCR analysis' results are shown in Figs. 6A–C. Among the genes related to I_{K1} and I_{to}, no gene has its expression, as measured by mRNA level, altered in *Gpc1*$^{-/-}$ as compared to CD1 mice strain. However, as many as four genes that relates to I_K are expressed in different levels in *Gpc1*$^{-/-}$ mice: *Kcng2*, *Kcnq1*, *Kcne1* and *Kcnh2*. These results support the functional data presented here as it will be discussed in the next section.

Discussion

The major finding of the present study is that the heparan sulfate proteoglycan Gpc1 is crucial to cardiac function. Our data strongly suggest that Gpc1 contributes to the membrane expression, as measured by K^+ current densities, and to the function of voltage-gated K^+ channels of ventricular cardiomyocytes, unquestionably affecting cardiac electrophysiology. Evident differences in the voltage gated K^+ currents between ventricular cardiomyocytes from CD1 and *Gpc1*$^{-/-}$ mice cannot be explained by the ventricular cardiomyocytes' heterogeneity and this matter will be further discussed in this section. The new knowledge presented here sets the stage for an innovative investigation of new modulators of the cardiac function, molecules that would interact specifically with Gpc1 and the glycosaminoglycans associated to it to regulate the cardiac function.

The heart fundamentally works as an intermittent pump to ultimately produce convection of the blood throughout the entire body. This blood convection transports oxygen and nutrients

to cells, and to move their wastes away from them [15]. Ventricular cardiomyocytes are all connected electrically in such a way that action potentials are propagated in three dimensions in the organ as electric excitation waves, the very ones picked up as ECG waves. Each cell has its own membrane elements and intracellular mechanisms to couple each intracellular action potential to a contractile event. The resting potential of a ventricular cardiomyocyte is stable, and it is governed mainly by leakage K^+ channels, inwardly rectifying K^+ channels (K_{ir}), that provides the K^+ currents I_{K1}. Upon receiving a suprathreshold depolarization stimulus through an electric synapse, voltage-gated Na^+ channels are activated, causing the membrane potential to reverse, reaching tens of millivolts positive inside the cell. Next, some voltage gated K^+ currents are activated briefly, generating the first repolarizing current, the I_{to}, crucially setting the membrane potential of the plateaued membrane potential during contraction as a next phase of the action potential. The plateaued membrane potential is basically a function of three rheogenic membrane events: i) slowly activating voltage-gated Ca^{2+} channels that provides a sustained inward Ca^{2+} current, ii) the rectification (decrease in conductance) of the channels that generate I_{K1}, and iii) reversion in Na^+-Ca^{2+} exchanger cycles contributing to additional Ca^{2+} entry. The plateau phase, period when contraction occurs, is terminated by the activation of another group of voltage gated K^+ channels, the delayed rectifiers, that provide the current I_K to fully repolarize the membrane potential. The delayed rectifiers are delayed by their voltage dependence and their biophysical properties such as their kinetics of activation and inactivation. Hence, the different classes of K^+ channels, each generating I_{K1}, I_{to} and I_K, are of utmost importance for the cardiac physiology.

K^+ channels determine the strength and the duration of cardiac contraction. In other words, they determine the cardiac output. Therefore, since we found a strong correlation between the presence of Gpc1, and the density and the properties of I_{to} and I_K currents in ventricular cardiomyocytes, we conclude that Gpc1, a HSPG, is a strong modulator of the cardiac activity.

Our data with *Gpc1*$^{-/-}$ mice revealed significant increase in cardiac stroke volume with preserved ejection fraction, yielding significantly increased cardiac output. *Gpc1*$^{-/-}$ mice also showed consistent abnormal ECG waves, particularly the QT and S-T segments. The QT interval is significantly delayed and 67% of the S-T segments are abnormal. In addition, T waves are also significantly delayed (Fig. 1 and Table 2). These two sets of data strongly indicate deficient repolarization at least in ventricular cardiomyocytes. With that in mind, we tested and showed, in isolated ventricular cardiomyocytes, action potentials taking longer to repolarize back to its resting potential with cells from *Gpc1*$^{-/-}$ compared to those from CD1 mice cells (Fig. 2). Hence, we focused on voltage-gated K^+ channels expressed by the ventricular cardiomyocytes as a possible molecular mechanism for the echocardiographic and electrocardiographic abnormalities in *Gpc1*$^{-/-}$ cardiac physiology. In fact, the association between changes in K^+ currents and cardiac remodeling is well-known, leading to cardiac arrhythmia, diastolic dysfunction, cardiac hypertrophy, and heart failure [16]–[19].

Sparse literature can be found regarding the influence of HSPG on the function of ion channels in general. Shear stress activates inward rectifier K^+ channel, $K_{ir}2.1$, in endothelial

cells by mechanisms that depend on the glycocalyx, an endothelial surface layer, rich in HSPG. This suggests a possible direct interaction of HSPG with an ion channel [6]. More recently, it has been shown that GAG modulate human H_v1 channels' gating properties with changes in voltage dependence [8]. Another work showed that Gpc3, by holding GAG within a 10 nm distance from the cell membrane, can interact with the Wnt1 membrane receptor (formerly *Int1* proto-oncogene) such as in hepatocellular carcinomas regulation [20]–[22] and in circulating tumor cells [23], evidencing direct interaction between Gpc3 and a membrane protein. It is very plausible to assume that extracellular molecules can interact with membrane proteins, such as ion channels, by inter molecular interactions as suggested by other studies [24], [25]. Based on our echocardiographic and electrocardiographic data, and the above-mentioned studies, we worked on the hypothesis that *Gpc1*$^{-/-}$ modulates voltage gated K^+ channels in the heart.

At first, we used a voltage clamp protocol consisting of 300 ms depolarizing pulses to different voltages, from a holding potential of −80 mV, to activate K^+ current by voltage, on isolated ventricular cardiomyocytes. This protocol was used without a conditioning pre-pulse to inactivate voltage gated Na^+ currents since that maneuver would also decrease the peak of K^+ current that is mostly I_{to} currents, of our interest. The duration of the pulse was chosen to cover 10-times the duration of the action potentials recorded in current clamp: approximately 30 ms (Fig. 2). We evaluated the peak of the K^+ currents as I_{to}, and the current amplitude at 300 ms as I_K, within what is commonly evaluated by peers [26], [27]. In fact, these previous studies represent I_{to} in mice ventricular cardiomyocytes as a transient outward current that is completely vanished (inactivated) after a 100-ms depolarization, hence at 300 ms timepoint I_{to} is totally gone. *Gpc1*$^{-/-}$ phenotype shows significantly depressed I_{to} (to 47%) and I_K (to 51%) as shown in Fig. 3. The currents, however, inactivate with statistically the same time constant, excluding the possibility of a simple inactivation kinetics process that would decrease the current level after 300-ms depolarizing pulse more intensively in *Gpc1*$^{-/-}$ ventricular cardiomyocytes (Supplementary Fig. 1). The third K^+ current that could interfere with the duration of the action potentials would be the I_{K1}, generated by leak channels selective to K^+, the inwardly rectifier channels. I_{K1} currents were unaltered in *Gpc1*$^{-/-}$ ventricular cardiomyocytes when compared to CD1 ventricular cardiomyocytes (Supplementary Fig. 2). I_{K1} currents from ventricular cardiomyocytes were mainly recorded during hyperpolarizing pulses from holding potential. At those potentials I_{to} and I_K are not active, therefore, besides leakage, I_{K1} currents are "isolated" from the other K^+ currents[28]–[30]. The decrease in I_{to} and I_K currents in *Gpc1*$^{-/-}$ cells to nearly a half of the amplitude in ventricular cardiomyocytes from CD1 mice could not be only explained by a randomly biased groups of ventricular cardiomyocytes. It is noteworthy to mention that our experiments included isolation of ventricular cardiomyocytes from a restricted area close to the apex of the ventricle (See methods). Thus, the group of cells utilized in this study is as homogeneous as possible being from the same region of the heart. Previous published studies have shown that cardiomyocytes isolated from the ventricular septum show nearly 50% reduction in I_{to} currents when compared to cardiomyocytes isolated from the ventricular apex region [27], [31]. Our data exclusively show recordings compatible with I_{to} currents isolated from the apex area, validating our specific isolation from apex ventricular cardiomyocytes. Therefore, we conclude that decreased currents are

part of the *Gpc1*$^{-/-}$ phenotype, and not produced by different populations of ventricular cardiomyocytes.

Next, we investigated the biophysical properties of the K^+ currents recorded from the ventricular cardiomyocytes from *Gpc1*$^{-/-}$ mice, seeking functional alterations in these currents. We investigated activation, inactivation, and recovery from inactivation of I_{to} and I_K voltage-activated K^+ currents.

The conductance activation by voltage both for I_{to} and I_K (See methods) were evaluated. The conductance activation by voltage for I_K, but not for I_{to}, showed a highly significant shift in voltage. I_K from CD1 mice ventricular cardiomyocytes showed a midpoint activation ($V_{1/2\text{-act}}$) at −3.55 mV on average. Meanwhile, I_K recorded from *Gpc1*$^{-/-}$ ventricular cardiomyocytes showed $V_{1/2\text{-act}}$ at +15.08 mV (See table 4 for details). These data denote an even more deficient repolarization phase due to much less K^+ current to repolarize the membrane during the action potential in those cells. The voltage sensitivity of the activation of I_{to} conductance was not significantly changed (Supplementary Fig. 3). A change in voltage-dependence as seen here for I_K, with a shift of more than 20 mV in the conductance curve, attest the significance of the data presented here. First, ventricular cardiomyocytes from different parts of the heart ventricle may have their K^+ conductance perhaps similarly changed in amplitude, but changes in the currents' voltage dependence has not been reported [18], [18], [31]–[33]. Second, we hypothesize that beyond a change in membrane expression of these proteins as indirectly induced by the absence of Gpc1, a different amount of heparan sulfate GAG may be in place since Gpc1 is one of the glypicans that has the GAG anchoring moieties the closest to the membrane, holding GAG negative charges close to the membrane, therefore close to the channels' extracellular surface. This feature is key for the interactions with other membrane proteins by changing the level of those membrane proteins surface charge screening [34]. It is well documented that charge screening, a possible interacting mechanism between GAG and ion channels, may change voltage dependence of voltage gated ion channels. As an example, pH, ionic strength and single charges near the voltage sensor of an ion channels are able to change the voltage-dependence of ion channels by simply biasing the voltage across the voltage sensors of these channels [35]–[39]. In fact, charge screening is also known to re-shape the protein surface, with functional consequences [40]. It remains to be determined whether charge screening is a major player in the regulation of cardiac K^+ channels by Gpc1 as a cause for the altered K^+ currents observed in *Gpc1*$^{-/-}$ mice cardiac phenotype, and this is a topic we will investigate in future studies.

We also interrogated the voltage-dependent inactivation of I_{to} and I_K currents. A pre-pulse was applied at different voltages and the non-inactivated current after that was evoked. Once again, I_{to} currents biophysical properties were not found altered in ventricular cardiomyocytes from *Gpc1*$^{-/-}$ mice. Differently, I_K showed the midpoint of inactivation ($V_{1/2\text{-inact}}$) at more negative pre-pulse voltages causing the inactivation curve to shift to more negative voltages accordingly, on average from −29.19 mV in CD1 cells to −46.84 mV in ventricular cardiomyocytes from *Gpc1*$^{-/-}$ mice (Fig. 4; Table 5). Maximal voltage sensitivity (coincident with maximal slope of the inactivation curve and the fraction of non-inactivated currents, were not altered in neither current case (Supplementary Fig. 4).

This almost 20 mV shift also attest that the channels are biophysically altered in *Gpc1*$^{-/-}$ ventricular cardiomyocytes as compared to cells from CD1 mice. This data corroborates the delayed repolarization of *Gpc1*$^{-/-}$ ventricular cardiomyocytes when in current clamp for action potentials recording.

The fact that $V_{1/2\text{-act}}$ and $V_{1/2\text{-inact}}$ are shifted in different directions for I_K from *Gpc1*$^{-/-}$ mice relative to data from CD1 allow us to speculate a mechanism on how the channels that relate to I_K are functionally altered. Most likely, the effects of Gpc1 on these channels are localized and we hypothesize it relates to a stabilization of a channel's voltage sensors states that are not in the deep resting but still not enough to gate-open the channel's pore. This hypothesis would explain the changes in the channels' activation and inactivation processes by voltage. Nevertheless, it was not the intention of this study to pinpoint a molecular mechanism for our findings. Interestingly, an elegant and seminal paper by the research group of Wonpil Im showed by molecular dynamics analysis that Gpc1 itself and heparan sulfate chains linked to it most likely interacts with other membrane proteins like K^+ channels, and this is definitely a line of investigation we will follow next [41]. It is perfectly possible that Gpc1 itself is able to reach extracellular moieties from membrane proteins and sustain a modulatory mechanism, since Gpc1 possesses an extensive unstructured C-terminal region that allows that required degree of freedom [42]. These possible interactions are still unexplored, and it represents a pathway for the next investigating steps regarding the altered cardiac function of *Gpc1*$^{-/-}$ hearts.

An important aspect of inactivation process in ion channels is the kinetics of recovery from inactivation, that reprimes channels to be activated again. *Gpc1*$^{-/-}$ mice ventricular cardiomyocytes showed remarkably different recovery from inactivation of both I_{to} and I_K currents. In *Gpc1*$^{-/-}$ ventricular cardiomyocytes, I_{to} recovered from inactivation with a time constant of 117 ms, considerably slower than in CD1 cells that do so in 75 ms (Fig. 5; Table 6). I_K currents, however, did recover from inactivation at similar speed in cells from both mice strains (Table 6). Moreover, the non-inactivated fraction of I_K currents has shown to be different between cells from the two mice strains (Figs. 5G–H). This parameter is originated either by channels that recover from inactivation within 10 ms (the shorter interpulse duration) or by a component that is not inactivated by the first 300 ms pulse to +60 mV. Despite its origin, in practice this parameter means the level of inactivation of I_K, but not I_{to}, is significantly changed from 89% of the total I_K in CD1 cells to 80% in *Gpc1*$^{-/-}$ cells, an approximate 10% change. This change amount adds up to other changes in I_K to delay action potentials repolarization in ventricular cardiomyocyte from *Gpc1*$^{-/-}$ mice.

Finally, we analyzed the transcription level of the genes encoding K^+ channels implicated in I_{K1}, I_{to} and I_K. We assessed the mRNA expression levels of an exhaustive list of targets that were selected based on recent studies of mice ventricular cardiomyocytes [10], [11].

In mice, K^+ channels subunits related to I_{K1} are channels sensitive to PIP2 (encoded by *Kcnj2* gene), coupled to G-protein (*Kcnj3* and *Kcnj5*) and the ones modulated by ATP/ADP ratio (*Kcnj5*, *Kcnj8*, *Kcnj11* and *Kcnj12*). Interestingly enough, none of these genes were shown to be transcribed differently when comparing ventricular samples from CD1 and *Gpc1*$^{-/-}$ mice. *Kcnj2* [43] and *Kcnj5* [44] are related to LQT syndrome and

could be responsible for alterations in ECG waves, however our data showing unaltered I_{K1} and unchanged gene transcription in *Gpc1*$^{-/-}$ mice do not support *Kcnj2* [43] and *Kcnj5* [44] as potential mediators of the changes in K^+ channels seen in *Gpc1*$^{-/-}$ ventricular cardiomyocytes.

I_{to} currents in mice are carried by ion channels formed by a smaller number of proteins, encoded by *Kcnd2*, *Kcnd3* and *Kcna7*. These ion channels are all voltage dependent and are named Kv4.2, Kv4.3 and Kv1.7, respectively. They are all low voltage activated and undergo fast inactivation so that the repolarization provided by I_{to} is brief and serves to set the stage (the membrane potential) for contraction onset. Despite a decrease in recorded I_{to} in *Gpc1*$^{-/-}$ relative to currents recorded in CD1 ventricular cardiomyocytes, these genes were not found differently expressed. This suggest that Gpc1 may regulate I_{to} by indirect mechanisms. Further experiments are needed to pinpoint possible associated signaling partners.

Delayed rectifiers, the channels that support I_K, are diverse. The genes that encode the subunits to co-assemble as homotetrameric channels are *Kcna5*, *Kcnb1*, *Kcnq* and *Kcnh2* that encodes K_v1. 5, Kv2.1, Kv7.1 and Kv11.1 (hERG in humans), respectively. *Kcne1*, that encodes minK, an important modulatory subunit for both Kv7.1 and Kv11.1, can also be considered part of I_K [15]. Importantly, the channels formed by Kv7.1 subunits when co-assembled with minK, feature a well-known activation kinetics that is apparently too slow for the time course of an action potential in a ventricular cardiomyocyte of a mouse. However, it has been elegantly demonstrated before that the targeted disruption of the *Kcnq1* gene in mice significantly delays the repolarization phase of the action potentials in ventricular cardiomyocytes[45]. The changes are observed both in electrocardiographic waves in living animals as well as in isolated cells. Besides, two overlooked genes appear as well expressed in mice ventricular cardiomyocytes: *Kcng2* and *Kcnv2*. The K^+ channels subunits encoded by these two genes do not form functional homotetrameric channels and therefore are named silent subunits. Despite that, the two subunits encoded by these genes, K_v6.2 and Kv8.2 are implicated in heterotetrameric voltage-gated K^+ channels when they co-express with Kv2.1. The final hybrid channels has inactivation properties different from those from homotetrameric Kv2.1 channels[46]. Our RT-qPCR analysis showed *Kcng2*, *Kcnq1* and *Kcnh2* transcripts significantly more abundantly transcribed. Ion channels are multimeric membrane proteins that have a biosynthetic pathway composed of several stages, with multiple regulatory proteins that can be regulated at various levels before insertion in the cell membrane [47]. Numerous studies have stated that genes encoding ion channels also have their expression in a heart cell influenced by the electrophysiology of the cell itself [48], [49]. For instance, in mice, dominant-negative knockout channels triggers upregulation of some genes for subunits for other channels seemingly as a compensatory mechanism [27], [50]. In the same direction, some ion channels blockers are enough to upregulate the expression of the gene for the same blocked channel in a clear short loop of positive feedback to compensate for the blocked channels. The case happens when mexiletine is used to block sodium channels [51]. In addition, I_K currents are regulated in the same short-loop-like way [52]. We conclude that the disparate between the lower amplitude of I_K and higher levels of pertaining genes transcriptions fit to this well described mechanism of compensation described above.

From our gene target list, the only gene significantly less transcribed in *Gpc1*$^{-/-}$ mice relative to CD1 mice was *Kcne1*. The protein encoded by *Kcne1*, minK, works as chaperone for channels formed by Kv7.1 or Kv11.1 subunits. It has been described that minK increases the half-life of these protein complexes in the endoplasmic reticulum, ultimately improving cell membrane expression [53], [54, p.]. MinK also have remarkable effects of K_v7.1 and K_v11.1 biophysics. In Kv7.1, MinK shifts voltage dependence of activation to more negative potentials and slows the kinetics of channels activation by two orders of magnitude [55]–[58]. In Kv11.1, MinK increase total current and shifts activation and inactivation to more negative voltages [59], [60]. Our findings demonstrate that I_K density is depressed in the membranes of ventricular cardiomyocytes from *Gpc1*$^{-/-}$ mice despite the fact that genes encoding the proteins that form the channels are more intensively transcribed (*Kcnq1* and *Kcnh2*) and less transcribed (*Kcne1*) as compared with data from ventricular cardiomyocytes from CD1 mice. Multiple alternative explanations are possible for the above. If we consider *Kcne1* transcription levels is reflected in minK protein synthesis, one would expect less current by downregulation of membrane targeting of channels formed by Kv7.1 and Kv11.1. However, the biophysical properties of I_K would be differently affected via Kv7.1 or Kv11.1 by minK. Our *Gpc1*$^{-/-}$ data show right shift in the voltage dependence of I_K activation and left shift in inactivation. Current activation by voltage is differently affected by minK on Kv7.1 (right shift) and Kv11.1 (left shift). In addition, we showed a more intense I_K inactivation after a 300 ms strong depolarization in *Gpc1*$^{-/-}$ ventricular cardiomyocytes. It is known that Kv7.1 channels co-expressed with minK as a complex have minimized inactivation, and that is quite consistent with our data for CD1 recovery from inactivation of I_K (Fig 5D) [61]. This rationale ultimately suggests *Gpc1*$^{-/-}$ ventricular cardiomyocytes may express less MinK as a complex with Kv7.1. Therefore, the Kv7.1 hypothesis that there may be less MinK expressed following less transcription of *Kcne1*, is more plausible. On the other hand, MinK greatly slows down Kv7.1 activation and that effect would certainly modify the total K^+ current profile in the first 300 ms depolarizing pulses used here. However, as stated before, the inactivation kinetics of the K^+ currents we recorded was unaltered in *Gpc1*$^{-/-}$ ventricular cardiomyocytes and in accordance with previous reports [62]. Therefore, further detailed investigation is necessary to fully elucidate the mechanisms above involved in the K^+ currents recorded from *Gpc1*$^{-/-}$ ventricular cardiomyocytes.

In summary, we show that the deletion of Gpc1, a HSPG, is strongly associated with mechanical dysfunction in the heart of mice. This knowledge strongly suggests Gpc1 and or, GAG as potential targets for therapeutics aiming at interfering with the cardiac function to reestablish normal function of the heart. Our data determines that voltage gated K^+ channels play a major role in the effects of Gpc1 on cardiac function. Our data sets the stage for a new avenue of investigation that will put the HSPG in the center of the development of new drugs and therapeutic approaches for cardiac function clinical and/or surgical intervention.

Methods

Ethical approval

All procedures involving animals were approved by University of Arizona institutional animal care and use committee – IACUC - approved under the protocols number 18–491 and 19–532, conformed to the Guide for the Care and Use of Laboratory Animals published by the US National Institutes of Health. The experiments were performed using 8 – 10 weeks old male CD1 (wild type) (Charles River Laboratories), and Gpc1 knockout (*Gpc1*$^{-/-}$). A breeding pair of *Gpc1*$^{-/-}$ was kindly donated by Dr. Arthur Lander (UC Irvine, CA) to AZC. This particular *Gpc1*$^{-/-}$ mice strain was developed in a CD1 genetic background which served as control experiments for comparison. During procedures, all necessary steps were taken to minimize animal pain and suffering. All the animals are maintained from the Animal Care Facility of The University of Arizona, Tucson, and housed in standard rodent cages, under a controlled 12-h light/12-h dark cycle at room temperature (23 ± 2°C).

Echocardiography measurement

Transthoracic echocardiography was performed. Mice were anesthetized via the intraperitoneal injection of ketamine (90mg/kg) and xylazine (10mg/kg). Zoomed two-dimensional (2D) images were used to determine a short-axis plane alignment in the transverse B-mode with the papillary muscles, and M-mode was then obtained for determining cardiac function level. Echocardiography was performed by The University of Arizona Phenotyping Core.

Electrocardiogram *In vivo*

Anesthesia in mice was induced with continuous 2% isoflurane (VetOne, Idaho, USA) into the induction chamber. Placed in the supine position with spontaneous breathing, over a heating pad constantly maintained the animal body temperature at 37 ± 0.5 °C. For electrocardiogram (ECG) recordings, three stainless steel electrodes were subcutaneously implanted. Signals from the ECG lead II was amplified using a DAM-80 AC Differential Amplifier (World Precision Instruments, Sarasota, FL, USA) and the amplified signal was low-pass filtered at 300 Hz with a 4-pole Bessel filter LPF-202A (Warner Instruments, Hamden, CT). Processed signal was then digitalized using a sampling frequency of 1 kHz (PowerLab 4/30, ADInstruments, Colorado, USA). Recordings were analyzed using LabChart 8 Pro software (AD Instruments, Colorado, USA). Heart rate, PR interval, QT interval, corrected QT interval (QTc), QRS complex, and T wave duration were measured using the average of 30 consecutive beats. QT interval was normalized for rodents using modified Bazett's equation $QTc(n)\text{-}B = QT/\sqrt{(RR/f)}$. Normalization factor (f) is the average duration of the RR interval of control mice [63], [64].

Myocyte isolation

Ventricular cardiomyocytes were isolated from male CD1 and *Gpc1*$^{-/-}$ mice by enzymatic digestion as described by Shioya with minor modifications [65]. Mice were sedated with continuous isoflurane, the thorax was opened and the heart was quickly and carefully removed, mounted in an aortic perfusion system (Langendorff technique) perfused with

cardiomyocyte isolation buffer (CIB) ((mM): 130 NaCl, 5.4 KCl, 0.5 $MgCl_2$, 0.33 NaH_2PO_4, 22 glucose, 25 HEPES, and 0.4 EGTA (pH 7,4)) containing collagenase type II (1 mg/mL) (Gibco, Invitrogen, Carlsbad, CA) protease type XIV (0.06 mg/mL) (Sigma-Aldrich, St. Louis, Missouri, USA) and trypsin (0,06 mg/mL) (Worthington Biochemical Corp. Lakewood, NJ, USA), at 37°C. After 9 minutes of perfusion, the heart was removed from the cannula, atria were disposed, and ventricles were separated. A piece of the left ventricle between the apex and septum was separated for ventricular cardiomyocytes isolation. Accordingly, the tissue was submitted to an additional 9 min of digestion at 37°C with CIB supplemented with the same concentration from collagenase type II, trypsin, protease type XIV, and 0.7 mM $CaCl_2$. The cells were isolated from the tissue through gentle agitation using a transfer pipette. The suspension of isolated cells was filtered with a fabric mesh and centrifuged at 1000 rpm for 30 s. The cells were resuspended and maintained in a CIB solution containing CaCl2 (1.2 mM) and serum bovine albumin (BSA, 2 mg/mL), for 10 min 37°C. Finally, the cells were centrifuged (1000 rpm for 30 s), the supernatant discarded, then and kept in Tyrode's solution with the following composition (in mM): 140 NaCl, 5.4 KCl, 0.5 MgCl2, 0.33 NaH2PO4, 22 glucose, 25 HEPES and 1.8 CaCl2 (pH 7.4). Cells were used for up to 4 hours after cell isolation.

Cellular electrophysiological whole-cell patch-clamp technique

Whole-cell voltage-clamp and current-clamp recordings were performed on individual ventricular cardiomyocytes at room temperature (18–20°C), using an Axopatch 200B amplifier (Molecular Devices, Sunnyvale, CA, USA). Recordings were filtered at 10 kHz and digitized at a sampling rate of 40 kHz. After achieving the whole-cell configuration, 2 to 3 min was waited to allow the establishment of an ionic equilibrium between the pipette solution and the intracellular environment. Series resistance was compensated at least at 70%, and recordings on cells that did not follow that criteria were removed from this study. Here we dealt with slow voltage-dependent processes, and the speed of the clamp in large cells as cardiomyocytes would not play a relevant role. In addition, existing deviations between the commanded voltage and the membrane potential would have similar effects on both CD1 and *Gpc1*$^{-/-}$ data. The recording electrodes had tip resistances of 1–3 MΩ. Data was analyzed using Clampfit 11.1 software (Molecular Devices, Sunnyvale, CA, USA). For the voltage clamp experiments, it was used a pipette solution with the following composition, in mM: 130 K-aspartate, 20 KCl, 2 $MgCl_2$, 5 NaCl, 5 EGTA, 10 HEPES and a bathing solution with the following composition, in mM: 130 NMDG, 5.6 KCl, 1.8 $CaCl_2$, 0.1 $CdCl_2$, 0.5 MgCl2, 11 glucose, 10 HEPES. Both voltage clamp solutions had the pH set to 7.4 before usage in the same day. During the voltage-clamp protocol, the holding potential was set at −70 mV.

I_{to} and I_K voltage gated K^+ currents were estimated from the peaks of the currents and after 300 ms from the depolarization onset, respectively. When necessary, the current values were transformed into conductance by Ohm's law.

Individual conductance-voltage (G-V) curves were normalized by their maxima and individually fitted with a Boltzmann equation in the form:

Health Research Alliance Author Manuscript

$$G(V_m) = \frac{1}{1 + e^{\frac{V_{1/2-act} - V_m}{slope}}}$$

where $G(V_m)$ is the conductance at a given membrane potential V_m, $V_{1/2-act}$ is the membrane potential where 50% of the conductance is active and the $slope$ is the voltage sensitivity of the G-V curve. Parameters $V_{1/2-act}$ and $slope$ were averaged and expressed as mean ± SEM.

Inactivation curves were performed with current values (peak and at 300-ms point) after conditioning prepulses varying from −100 mV to +50 mV, for 300 ms, in the series. Individual curves were equally fitted with the Boltzmann equation in the form:

$$I(V_{p-p}) = \frac{1}{1 + e^{\frac{V_{1/2-inact} - V_m}{slope}}}$$

where $I(V_{p-p})$ is the available current at a given V_{p-p}, $V_{1/2-inact}$ is the membrane potential at the pre-pulse where 50% of the currents are inactivated and the $slope$ is the voltage sensitivity of the curve. Parameters $V_{1/2-inact}$ and $slope$ were averaged and expressed as mean ± SEM.

Voltage-activated K^+ currents decays over 300-ms depolarizing pulses were fitted by single exponentials using no constrains. The generalized equation is as follows:

$$Y = (Y0 - Plateau) \times e^{\frac{-t}{\tau}} + Plateau$$

Where Y is the current value at any point in time, $Y0$ is the current at $t = 0$, τ is the time constant of the inactivation process and the $Plateau$ is the asymptotic value after many time constants, typically five.

Recovery from inactivation was studied with a triple-pulse protocol, with the first pulse at +60mV and lasting 300 ms, a second pulse lasting 10–1010 ms (varying at 100 ms), and a third pulse at +60mV lasting 300 ms as well. The ratio of currents between third and first pulse was plotted, individually, against the duration of the second pulse. Individual data was fitted with a single exponential. The time constant and the current amplitude related to the 10-ms second pulse (named non-inactivated fraction) were averaged and expressed as mean ± SEM.

For current-clamp mode experiments, intended for action potential (AP) recordings, pipettes were filled with an internal solution composed of (mM): 20 KCl, 130 K-aspartate, 130 KOH, 10 HEPES, 2 $MgCl_2$, 5 NaCl, pH set to 7.2 using KOH. In all current-clamp recordings, cells were bathed with the Tyrode solution composed of, in mM: 132 NaCl, 4 KCl, 1.8 CaCl2, 1.2 MgCl2, 5.5, glucose and 10 HEPES and pH set to 7.4 with NaOH. After the establishment of the whole-cell configuration, the recording mode was immediately switched to the current-clamp mode, and resting membrane potential was measured.

Ventricular cardiomyocytes' action potentials were evoked by injecting depolarizing current with the patch pipette, with amplitudes of 200 – 300 pA and 2–3 ms duration.

Quantitative real-time PCR experiments

The ventricle tissues collected were used for total RNA extraction by TRIZOL® (Invitrogen, CA, USA), and quantified using NanoDrop (Thermo Fisher Scientific, MA, USA). Quantitative polymerase chain reaction (qPCR) was performed using Power SYBR™ Green RNA to CT™ RT-PCR kit (Applied Biosystems by Thermo Fisher Scientific), according to manufacturer's guidance method. The specific primers (Supplementary Table 1) were obtained from Integrated DNA Technologies (IDT). Gene expression was normalized by the housekeeping gene *Eef1e1*[14], and expressed as $2^{-\Delta\Delta Ct}$.

Statistical analysis

Statistical analyses were performed using GraphPad Prism 8 (San Diego, CA, USA). Data are presented as the mean ± S.E.M unless when indicated. Statistical significance between groups was performed using Student's t-test (unpaired) and one-way ANOVA with Bonferroni *post hoc* testing. For comparison of abnormal ST-segment, a 2×2 contingency table using the Chi-square test without Yates correction was used. Differences were considered to be statistically significant when $P < 0.05$.

Supplementary Material

Refer to Web version on PubMed Central for supplementary material.

Funding:

This study was supported by funds from the Department of Anesthesiology at the University of Arizona and by the American Heart Association (CDA Grant # 850700/2021 [AZC]).

References

[1]. Hansen M, Garcia R, Dull RO, Carvalho-de-Souza JL, and Chignalia AZ, "Glypican-1 and Remodeling Cardiac Hypertrophy.," The FASEB Journal, vol. 34, no. S1, pp. 1–1, 2020, doi: 10.1096/fasebj.2020.34.s1.05765.

[2]. S. R. Potje et al. , "Glypican 1 and syndecan 1 differently regulate noradrenergic hypertension development: focus on IP3R and calcium," Pharmacol Res, p. 105813, Aug. 2021, doi: 10.1016/j.phrs.2021.105813. [PubMed: 34411733]

[3]. Filmus J, Capurro M, and Rast J, "Glypicans," Genome Biol, vol. 9, no. 5, p. 224, 2008, doi: 10.1186/gb-2008-9-5-224. [PubMed: 18505598]

[4]. Wang S, Qiu Y, and Bai B, "The Expression, Regulation, and Biomarker Potential of Glypican-1 in Cancer," Front Oncol, vol. 9, p. 614, 2019, doi: 10.3389/fonc.2019.00614. [PubMed: 31355137]

[5]. Wang W et al. , "Assembling custom side chains on proteoglycans to interrogate their function in living cells," Nat Commun, vol. 11, no. 1, p. 5915, Nov. 2020, doi: 10.1038/s41467-020-19765-y. [PubMed: 33219207]

[6]. Fancher IS et al. , "Impairment of Flow-Sensitive Inwardly Rectifying K+ Channels via Disruption of Glycocalyx Mediates Obesity-Induced Endothelial Dysfunction," Arterioscler Thromb Vasc Biol, vol. 40, no. 9, pp. e240–e255, Sep. 2020, doi: 10.1161/ATVBAHA.120.314935. [PubMed: 32698687]

[7]. Ahn SJ, Le Master E, Lee JC, Phillips SA, Levitan I, and Fancher IS, "Differential effects of obesity on visceral versus subcutaneous adipose arteries: role of shear-activated Kir2.1 and

alterations to the glycocalyx," Am J Physiol Heart Circ Physiol, vol. 322, no. 2, pp. H156–H166, Feb. 2022, doi: 10.1152/ajpheart.00399.2021. [PubMed: 34890278]

[8]. Orts DJB and Arcisio-Miranda M, "Cell glycosaminoglycans content modulates human voltage-gated proton channel (HV 1) gating," FEBS J, Nov. 2021, doi: 10.1111/febs.16290.

[9]. Harrell MD, Harbi S, Hoffman JF, Zavadil J, and Coetzee WA, "Large-scale analysis of ion channel gene expression in the mouse heart during perinatal development," Physiol Genomics, vol. 28, no. 3, pp. 273–283, Feb. 2007, doi: 10.1152/physiolgenomics.00163.2006. [PubMed: 16985003]

[10]. Chevalier M, Vermij SH, Wyler K, Gillet L, Keller I, and Abriel H, "Transcriptomic analyses of murine ventricular cardiomyocytes," Sci Data, vol. 5, p. 180170, Aug. 2018, doi: 10.1038/sdata.2018.170. [PubMed: 30129933]

[11]. Iacobas S, Amuzescu B, and Iacobas DA, "Transcriptomic uniqueness and commonality of the ion channels and transporters in the four heart chambers," Sci Rep, vol. 11, no. 1, p. 2743, Feb. 2021, doi: 10.1038/s41598-021-82383-1. [PubMed: 33531573]

[12]. Flenner F et al. , "Translational investigation of electrophysiology in hypertrophic cardiomyopathy," J Mol Cell Cardiol, vol. 157, pp. 77–89, Aug. 2021, doi: 10.1016/j.yjmcc.2021.04.009. [PubMed: 33957110]

[13]. Joukar S, "A comparative review on heart ion channels, action potentials and electrocardiogram in rodents and human: extrapolation of experimental insights to clinic," Lab Anim Res, vol. 37, no. 1, p. 25, Sep. 2021, doi: 10.1186/s42826-021-00102-3. [PubMed: 34496976]

[14]. Ruiz-Villalba A, Mattiotti A, Gunst QD, Cano-Ballesteros S, van den Hoff MJB, and Ruijter JM, "Reference genes for gene expression studies in the mouse heart," Sci Rep, vol. 7, no. 1, p. 24, Feb. 2017, doi: 10.1038/s41598-017-00043-9. [PubMed: 28154421]

[15]. Boron WF and Boulpaep EL, Eds., Medical physiology, Third edition. Philadelphia, PA: Elsevier, 2017.

[16]. Näbauer M and Kääb S, "Potassium channel down-regulation in heart failure," Cardiovasc Res, vol. 37, no. 2, pp. 324–334, Feb. 1998, doi: 10.1016/S0008-6363(97)00274-5. [PubMed: 9614489]

[17]. Chen L, Sampson KJ, and Kass RS, "Cardiac Delayed Rectifier Potassium Channels in Health and Disease," Card Electrophysiol Clin, vol. 8, no. 2, pp. 307–322, Jun. 2016, doi: 10.1016/j.ccep.2016.01.004. [PubMed: 27261823]

[18]. Grandi E et al. , "Potassium channels in the heart: structure, function and regulation," The Journal of Physiology, vol. 595, no. 7, pp. 2209–2228, Apr. 2017, doi: 10.1113/JP272864. [PubMed: 27861921]

[19]. Abraham DM et al. , "The two-pore domain potassium channel TREK-1 mediates cardiac fibrosis and diastolic dysfunction," J Clin Invest, vol. 128, no. 11, pp. 4843–4855, Nov. 2018, doi: 10.1172/JCI95945. [PubMed: 30153110]

[20]. Capurro MI, Xiang Y-Y, Lobe C, and Filmus J, "Glypican-3 promotes the growth of hepatocellular carcinoma by stimulating canonical Wnt signaling," Cancer Res, vol. 65, no. 14, pp. 6245–6254, Jul. 2005, doi: 10.1158/0008-5472.CAN-04-4244. [PubMed: 16024626]

[21]. Gao W and Ho M, "The role of glypican-3 in regulating Wnt in hepatocellular carcinomas," Cancer Rep, vol. 1, no. 1, pp. 14–19, 2011. [PubMed: 22563565]

[22]. Niehrs C, "The complex world of WNT receptor signalling," Nat Rev Mol Cell Biol, vol. 13, no. 12, pp. 767–779, Dec. 2012, doi: 10.1038/nrm3470. [PubMed: 23151663]

[23]. Ahrens TD et al. , "The Role of Proteoglycans in Cancer Metastasis and Circulating Tumor Cell Analysis," Front Cell Dev Biol, vol. 8, p. 749, 2020, doi: 10.3389/fcell.2020.00749. [PubMed: 32984308]

[24]. Tang W, Ruknudin A, Yang WP, Shaw SY, Knickerbocker A, and Kurtz S, "Functional expression of a vertebrate inwardly rectifying K+ channel in yeast," Mol Biol Cell, vol. 6, no. 9, pp. 1231–1240, Sep. 1995, doi: 10.1091/mbc.6.9.1231. [PubMed: 8534918]

[25]. Minor DL, Masseling SJ, Jan YN, and Jan LY, "Transmembrane structure of an inwardly rectifying potassium channel," Cell, vol. 96, no. 6, pp. 879–891, Mar. 1999, doi: 10.1016/s0092-8674(00)80597-8. [PubMed: 10102275]

[26]. Brouillette J, Clark RB, Giles WR, and Fiset C, "Functional properties of K+ currents in adult mouse ventricular myocytes," J Physiol, vol. 559, no. Pt 3, pp. 777–798, Sep. 2004, doi: 10.1113/jphysiol.2004.063446. [PubMed: 15272047]

[27]. Guo W, Xu H, London B, and Nerbonne JM, "Molecular basis of transient outward K+ current diversity in mouse ventricular myocytes," J Physiol, vol. 521 Pt 3, pp. 587–599, Dec. 1999, doi: 10.1111/j.1469-7793.1999.00587.x. [PubMed: 10601491]

[28]. Santos-Miranda A, Cruz JS, and Roman-Campos D, "Electrical properties of isolated cardiomyocytes in a rat model of thiamine deficiency," Arq Bras Cardiol, vol. 104, no. 3, pp. 242–245, Mar. 2015, doi: 10.5935/abc.20150010. [PubMed: 25884771]

[29]. Karle CA et al. , "Human cardiac inwardly-rectifying K+ channel Kir(2.1b) is inhibited by direct protein kinase C-dependent regulation in human isolated cardiomyocytes and in an expression system," Circulation, vol. 106, no. 12, pp. 1493–1499, Sep. 2002, doi: 10.1161/01.cir.0000029747.53262.5c. [PubMed: 12234954]

[30]. Zobel C et al. , "Molecular dissection of the inward rectifier potassium current (IK1) in rabbit cardiomyocytes: evidence for heteromeric co-assembly of Kir2.1 and Kir2.2," J Physiol, vol. 550, no. Pt 2, pp. 365–372, Jul. 2003, doi: 10.1113/jphysiol.2002.036400. [PubMed: 12794173]

[31]. Xu H, Guo W, and Nerbonne JM, "Four kinetically distinct depolarization-activated K+ currents in adult mouse ventricular myocytes," J Gen Physiol, vol. 113, no. 5, pp. 661–678, May 1999, doi: 10.1085/jgp.113.5.661. [PubMed: 10228181]

[32]. Tristani-Firouzi M, Chen J, Mitcheson JS, and Sanguinetti MC, "Molecular biology of K(+) channels and their role in cardiac arrhythmias," Am J Med, vol. 110, no. 1, pp. 50–59, Jan. 2001, doi: 10.1016/s0002-9343(00)00623-9. [PubMed: 11152866]

[33]. Nerbonne JM and Guo W, "Heterogeneous expression of voltage-gated potassium channels in the heart: roles in normal excitation and arrhythmias," J Cardiovasc Electrophysiol, vol. 13, no. 4, pp. 406–409, Apr. 2002, doi: 10.1046/j.1540-8167.2002.00406.x. [PubMed: 12033361]

[34]. Matsuda K et al. , "Glypican-1 Is Overexpressed in Human Breast Cancer and Modulates the Mitogenic Effects of Multiple Heparin-binding Growth Factors in Breast Cancer Cells," Cancer Res, vol. 61, no. 14, pp. 5562–5569, Jul. 2001. [PubMed: 11454708]

[35]. Hartzell HC and White RE, "Effects of magnesium on inactivation of the voltage-gated calcium current in cardiac myocytes," J Gen Physiol, vol. 94, no. 4, pp. 745–767, Oct. 1989, doi: 10.1085/jgp.94.4.745. [PubMed: 2559140]

[36]. Islas LD and Sigworth FJ, "Electrostatics and the Gating Pore of Shaker Potassium Channels," J Gen Physiol, vol. 117, no. 1, pp. 69–90, Jan. 2001. [PubMed: 11134232]

[37]. Starace DM and Bezanilla F, "Histidine scanning mutagenesis of basic residues of the S4 segment of the shaker k+ channel," J Gen Physiol, vol. 117, no. 5, pp. 469–490, May 2001, doi: 10.1085/jgp.117.5.469. [PubMed: 11331357]

[38]. Trapani JG and Korn SJ, "Effect of External pH on Activation of the Kv1.5 Potassium Channel," Biophys J, vol. 84, no. 1, pp. 195–204, Jan. 2003. [PubMed: 12524275]

[39]. Villalba-Galea CA, Frezza L, Sandtner W, and Bezanilla F, "Sensing charges of the Ciona intestinalis voltage-sensing phosphatase," J. Gen. Physiol, vol. 142, no. 5, pp. 543–555, Nov. 2013, doi: 10.1085/jgp.201310993. [PubMed: 24127524]

[40]. Wilson DL, Morimoto K, Tsuda Y, and Brown AM, "Interaction between calcium ions and surface charge as it relates to calcium currents," J Membr Biol, vol. 72, no. 1–2, pp. 117–130, 1983, doi: 10.1007/BF01870319. [PubMed: 6304316]

[41]. Dong C et al. , "Structure, Dynamics, and Interactions of GPI-Anchored Human Glypican-1 with Heparan Sulfates in a Membrane," Glycobiology, vol. 31, no. 5, pp. 593–602, Jun. 2021, doi: 10.1093/glycob/cwaa092. [PubMed: 33021626]

[42]. Svensson G, Awad W, Håkansson M, Mani K, and Logan DT, "Crystal structure of N-glycosylated human glypican-1 core protein: structure of two loops evolutionarily conserved in vertebrate glypican-1," J Biol Chem, vol. 287, no. 17, pp. 14040–14051, Apr. 2012, doi: 10.1074/jbc.M111.322487. [PubMed: 22351761]

[43]. Eckhardt LL et al. , "KCNJ2 mutations in arrhythmia patients referred for LQT testing: a mutation T305A with novel effect on rectification properties," Heart Rhythm, vol. 4, no. 3, pp. 323–329, Mar. 2007, doi: 10.1016/j.hrthm.2006.10.025. [PubMed: 17341397]

[44]. Wang F et al. , “The phenotype characteristics of type 13 long QT syndrome with mutation in KCNJ5 (Kir3.4-G387R),” Heart Rhythm, vol. 10, no. 10, pp. 1500–1506, Oct. 2013, doi: 10.1016/j.hrthm.2013.07.022. [PubMed: 23872692]

[45]. Casimiro MC et al. , “Targeted disruption of the Kcnq1 gene produces a mouse model of Jervell and Lange-Nielsen Syndrome,” Proc Natl Acad Sci U S A, vol. 98, no. 5, pp. 2526–2531, Feb. 2001, doi: 10.1073/pnas.041398998. [PubMed: 11226272]

[46]. Bocksteins E and Snyders DJ, “Electrically silent Kv subunits: their molecular and functional characteristics,” Physiology (Bethesda), vol. 27, no. 2, pp. 73–84, Apr. 2012, doi: 10.1152/physiol.00023.2011. [PubMed: 22505664]

[47]. Deutsch C, “The Birth of a Channel,” Neuron, vol. 40, no. 2, pp. 265–276, Oct. 2003, doi: 10.1016/S0896-6273(03)00506-3. [PubMed: 14556708]

[48]. Rosati B and McKinnon D, “Regulation of ion channel expression,” Circ Res, vol. 94, no. 7, pp. 874–883, Apr. 2004, doi: 10.1161/01.RES.0000124921.81025.1F. [PubMed: 15087427]

[49]. Balse E, Steele DF, Abriel H, Coulombe A, Fedida D, and Hatem SN, “Dynamic of ion channel expression at the plasma membrane of cardiomyocytes,” Physiol Rev, vol. 92, no. 3, pp. 1317–1358, Jul. 2012, doi: 10.1152/physrev.00041.2011. [PubMed: 22811429]

[50]. Guo W, Li H, London B, and Nerbonne JM, “Functional consequences of elimination of i(to,f) and i(to,s): early afterdepolarizations, atrioventricular block, and ventricular arrhythmias in mice lacking Kv1.4 and expressing a dominant-negative Kv4 alpha subunit,” Circ Res, vol. 87, no. 1, pp. 73–79, Jul. 2000, doi: 10.1161/01.res.87.1.73. [PubMed: 10884375]

[51]. Duff HJ, Offord J, West J, and Catterall WA, “Class I and IV antiarrhythmic drugs and cytosolic calcium regulate mRNA encoding the sodium channel alpha subunit in rat cardiac muscle,” Mol Pharmacol, vol. 42, no. 4, pp. 570–574, Oct. 1992. [PubMed: 1331749]

[52]. Zhou J, Kodirov S, Murata M, Buckett PD, Nerbonne JM, and Koren G, “Regional upregulation of Kv2.1-encoded current, IK,slow2, in Kv1DN mice is abolished by crossbreeding with Kv2DN mice,” Am J Physiol Heart Circ Physiol, vol. 284, no. 2, pp. H491–500, Feb. 2003, doi: 10.1152/ajpheart.00576.2002. [PubMed: 12529256]

[53]. Peroz D, Dahimène S, Baró I, Loussouarn G, and Mérot J, “LQT1-associated mutations increase KCNQ1 proteasomal degradation independently of Derlin-1,” J Biol Chem, vol. 284, no. 8, pp. 5250–5256, Feb. 2009, doi: 10.1074/jbc.M806459200. [PubMed: 19114714]

[54]. Roura-Ferrer M et al. , “Impact of KCNE subunits on KCNQ1 (Kv7.1) channel membrane surface targeting,” J Cell Physiol, vol. 225, no. 3, pp. 692–700, Nov. 2010, doi: 10.1002/jcp.22265. [PubMed: 20533308]

[55]. Barhanin J, Lesage F, Guillemare E, Fink M, Lazdunski M, and Romey G, “K v LQT1 and IsK (minK) proteins associate to form the I KS cardiac potassium current,” Nature, vol. 384, no. 6604, Art. no. 6604, Nov. 1996, doi: 10.1038/384078a0.

[56]. Tapper AR and George AL, “Location and orientation of minK within the I(Ks) potassium channel complex,” J Biol Chem, vol. 276, no. 41, pp. 38249–38254, Oct. 2001, doi: 10.1074/jbc.M103956200. [PubMed: 11479291]

[57]. Meisel E, Tobelaim W, Dvir M, Haitin Y, Peretz A, and Attali B, “Inactivation gating of Kv7.1 channels does not involve concerted cooperative subunit interactions,” Channels (Austin), vol. 12, no. 1, pp. 89–99, Jan. 2018, doi: 10.1080/19336950.2018.1441649. [PubMed: 29451064]

[58]. Wang Y, Eldstrom J, and Fedida D, “Gating and Regulation of KCNQ1 and KCNQ1 + KCNE1 Channel Complexes,” Front Physiol, vol. 11, p. 504, 2020, doi: 10.3389/fphys.2020.00504. [PubMed: 32581825]

[59]. McDonald TV et al. , “A minK-HERG complex regulates the cardiac potassium current I(Kr),” Nature, vol. 388, no. 6639, pp. 289–292, Jul. 1997, doi: 10.1038/40882. [PubMed: 9230439]

[60]. Anantharam A and Abbott GW, “Does hERG coassemble with a beta subunit? Evidence for roles of MinK and MiRP1,” Novartis Found Symp, vol. 266, pp. 100–112; discussion 112–117, 155–158, 2005. [PubMed: 16050264]

[61]. Tristani-Firouzi M and Sanguinetti MC, “Voltage-dependent inactivation of the human K+ channel KvLQT1 is eliminated by association with minimal K+ channel (minK) subunits,” J Physiol, vol. 510 (Pt 1), pp. 37–45, Jul. 1998, doi: 10.1111/j.1469-7793.1998.037bz.x. [PubMed: 9625865]

Health Research Alliance Author Manuscript

[62]. Choi B-R et al. , “Transient Outward K+ Current (Ito) Underlies the Right Ventricular Initiation of Polymorphic Ventricular Tachycardia in a Transgenic Rabbit Model of Long-QT Syndrome Type 1,” Circ Arrhythm Electrophysiol, vol. 11, no. 6, p. e005414, Jun. 2018, doi: 10.1161/CIRCEP.117.005414. [PubMed: 29769222]

[63]. Gondim ANS et al. , “(−)-Terpinen-4-ol changes intracellular Ca2+ handling and induces pacing disturbance in rat hearts,” European Journal of Pharmacology, vol. 807, pp. 56–63, Jul. 2017, doi: 10.1016/j.ejphar.2017.04.022. [PubMed: 28435092]

[64]. Kmecova J and Klimas J, “Heart rate correction of the QT duration in rats,” Eur. J. Pharmacol, vol. 641, no. 2–3, pp. 187–192, Sep. 2010, doi: 10.1016/j.ejphar.2010.05.038. [PubMed: 20553920]

[65]. Shioya T, “A simple technique for isolating healthy heart cells from mouse models,” J Physiol Sci, vol. 57, no. 6, pp. 327–335, Dec. 2007, doi: 10.2170/physiolsci.RP010107. [PubMed: 17980092]

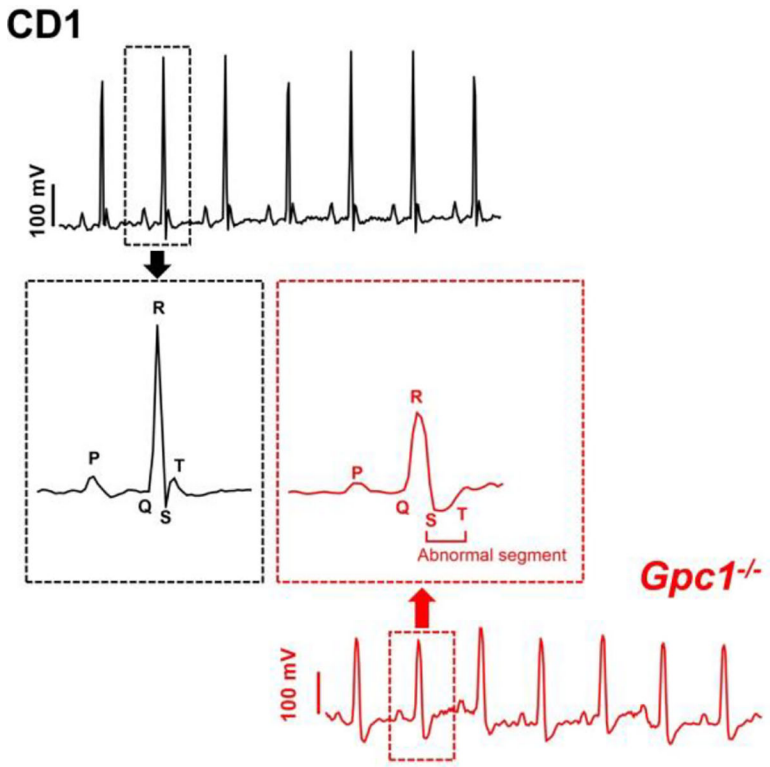

Figure 1. Electrocardiographic recordings in *Gpc1*$^{-/-}$ mice.

Typical electrocardiogram recordings in CD1 mice (top panels in black) and *Gpc1*$^{-/-}$ mice (bottom panels in red). The middle inserts show typical P-QRS-T complexes from our recordings, and they evidence the differences in the S-T segments and T waves from the two different mice strains.

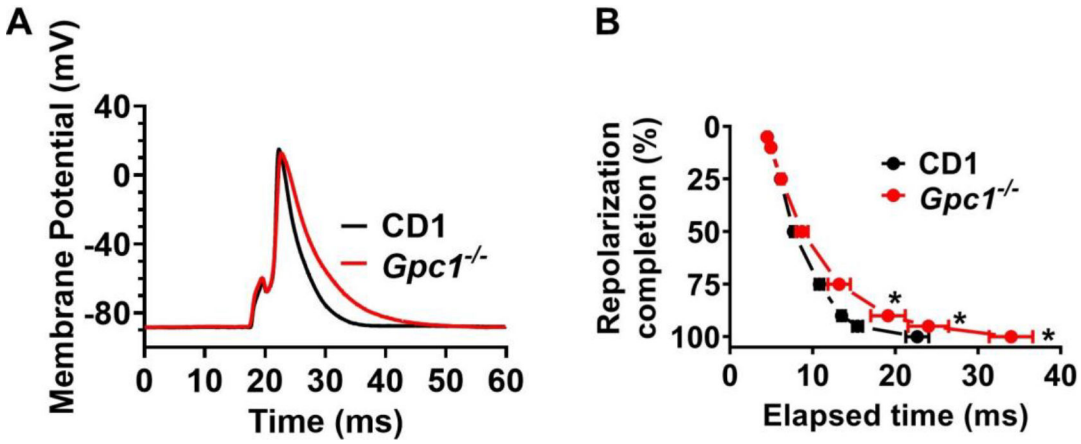

Figure 2. Action potentials from *Gpc1*$^{-/-}$ mice ventricular cardiomyocytes feature delayed repolarization.

A. Representative action potentials recorded in CD1 mice (black) and *Gpc1*$^{-/-}$ mice (red). In both cases the activity was elicited by a 3 ms 400 pA current depolarizing stimuli delivered by the patch pipette. **B**. shows the average ± S.E.M (n=10 for CD1 and n=11 for *Gpc1*$^{-/-}$ datasets) elapsed time for repolarization after the stimuli onset.

*Denotes $p < 0.05$ when comparing CD1 *vs Gpc1*$^{-/-}$with unpaired Student's t-test. (For interpretation of the references to colour in this figure legend, the reader is referred to the web version of this article.)

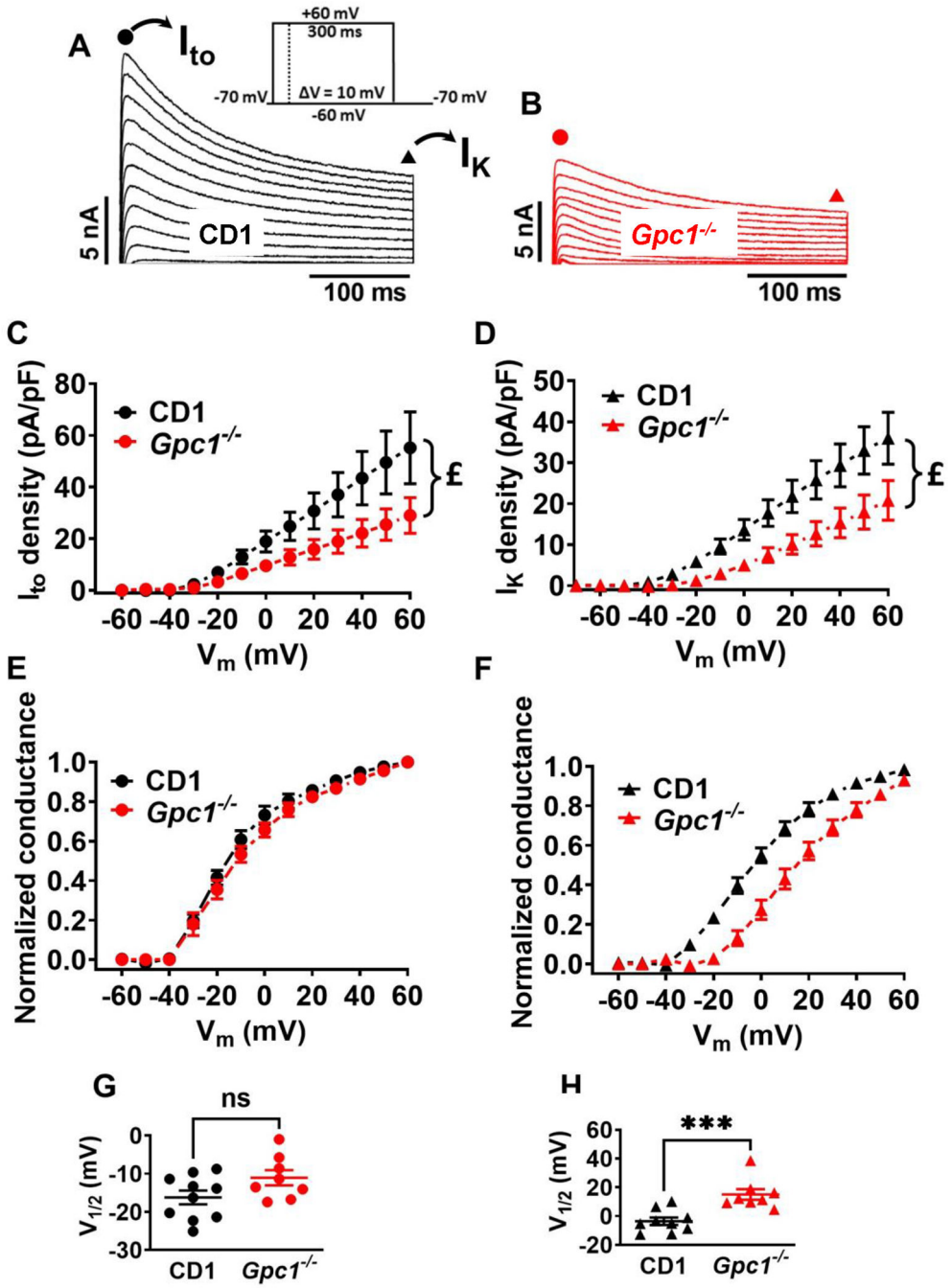

Figure 3. Voltage-activated K^+ currents in ventricular cardiomyocytes from CD1 and *Gpc1*$^{-/-}$ mice.

A and **B**, typical voltage-activated K^+ currents recorded in voltage-clamped (protocol in the inset) ventricular cardiomyocytes from CD1 (**A**, black) and *Gpc1*$^{-/-}$ (**B**, red) mice are shown (see methods section for details). Transient outward K^+ currents (I_{to}) were taken from the peak of the recorded currents (circles) delay rectifier K^+ currents (I_K) were taken at the end of a 300 ms depolarizing pulse (triangles). **C** and **D**, currents values were normalized by the cell capacitance before the generation of a current–voltage (I-V) curves by plotting the

current densities against the membrane potential V_m. CD1 *vs* *Gpc1*$^{-/-}$ data comparison for I_{to} (**C**) and for I_K (**D**) showed statistical difference, indicated by "£" with P<0.001 (Two-way ANOVA). **E** and **F**, current values were transformed into conductance by the Ohm's law to generate conductance-voltage (G-V) curves, normalized by its maxima in the same cell, averaged and plotted against V_m. Each individual G-V curve was fitted with Boltzmann equation (see methods) and generated a $V_{1/2}$ and a slope. Note the clear shift in the data plotted in **F** that is the voltage dependence for the conductance that generates I_K. **G** and **H**, statistical analysis of $V_{1/2}$ from different current and mice strains showed only in the case of I_K there was a statistical difference when data from CD1 and *Gpc1*$^{-/-}$ are compared. Slope data were not different. All plotted data are presented as means ± S.E.M. (n = 8–9). ***Denotes p < 0.001 when tested with unpaired Student's t-test. (For interpretation of the references to colour in this figure legend, the reader is referred to the web version of this article.)

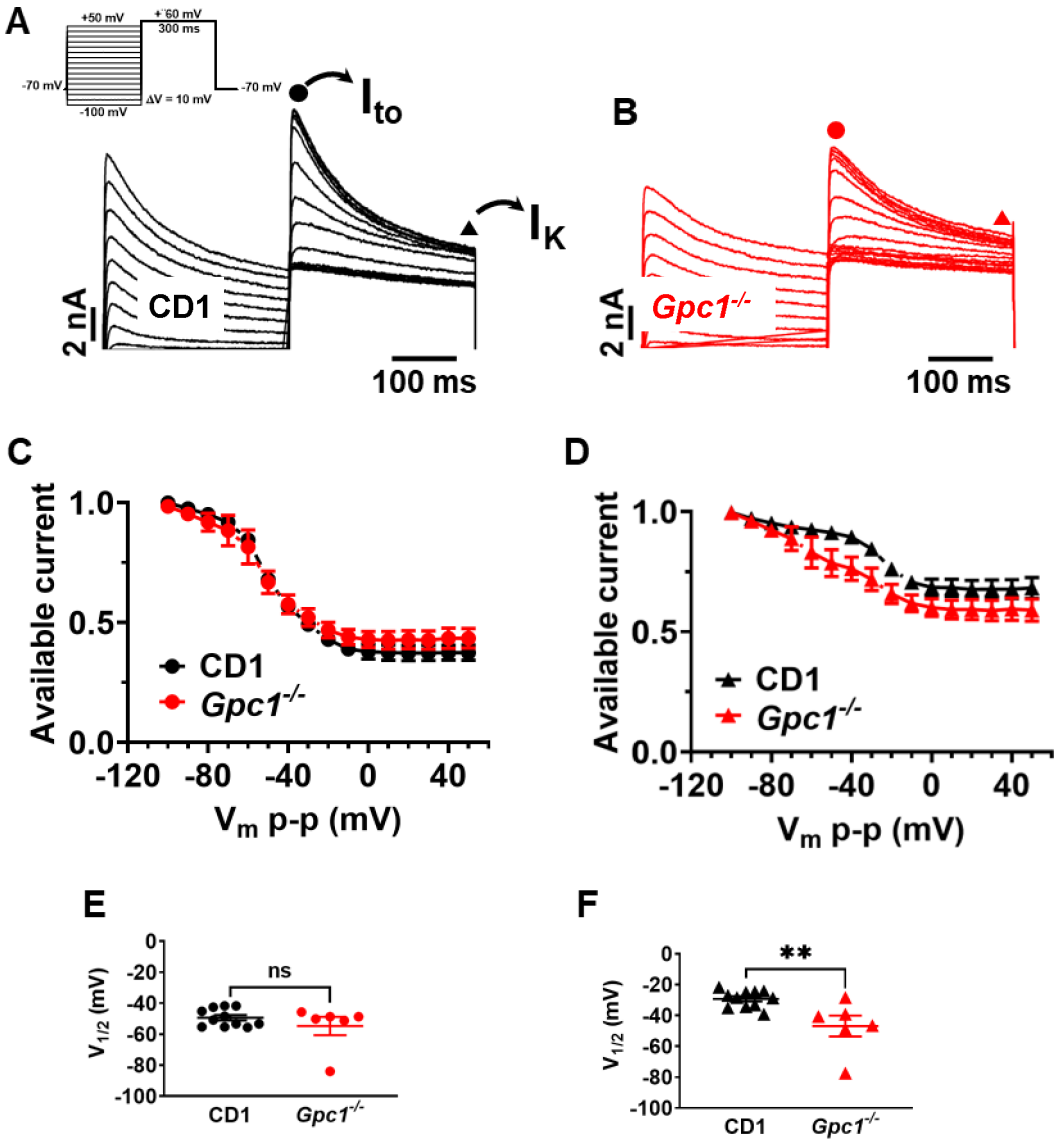

Figure 4. Steady-state inactivation of I_{to} and I_K in ventricular myocytes from CD1 mice and *Gpc1*$^{-/-}$ mice.

A and **B**, typical current traces recorded in voltage-clamped (protocol in the inset) for the study of inactivation of I_{to} and I_K in ventricular cardiomyocytes from CD1 (**A**, black) and *Gpc1*$^{-/-}$ (**B**, red) mice (see methods section for details). Transient outward K^+ currents (I_{to}) were taken from the peak of the recorded currents (circles) delay rectifier K^+ currents (I_K) were taken at the end of a 300 ms depolarizing pulse (triangles) and indicated in the figure. **C** and **D**, individual datasets (same cell) for I_{to} (**C**) and I_K (**D**) were normalized by its maxima, averaged, and plotted against the membrane potential during the conditioning pre-pulse (V_mp-p). Note that the inactivation of I_K showed in **D** is clearly shifted to more negative V_mp-p values. Individual inactivation curves were fitted with the Boltzmann's formalism (see methods) to generate a $V_{1/2\text{-inact}}$ that is the conditioning voltage that inactivates 50% of the inactivating current, a slope of the curve and a level of non-inactivating currents after the 300 ms conditioning period. **E** and **F**, statistical analysis

Health Research Alliance Author Manuscript

of $V_{1/2\text{-inact}}$ from different current and mice strains showed only in the case of I_K there was a statistical difference when data from CD1 and *Gpc1*$^{-/-}$ are compared. All plotted data are presented as means ± S.E.M. (n = 8–10). **Denotes $P < 0.01$ when tested with unpaired Student's t-test. (For interpretation of the references to colour in this figure legend, the reader is referred to the web version of this article.)

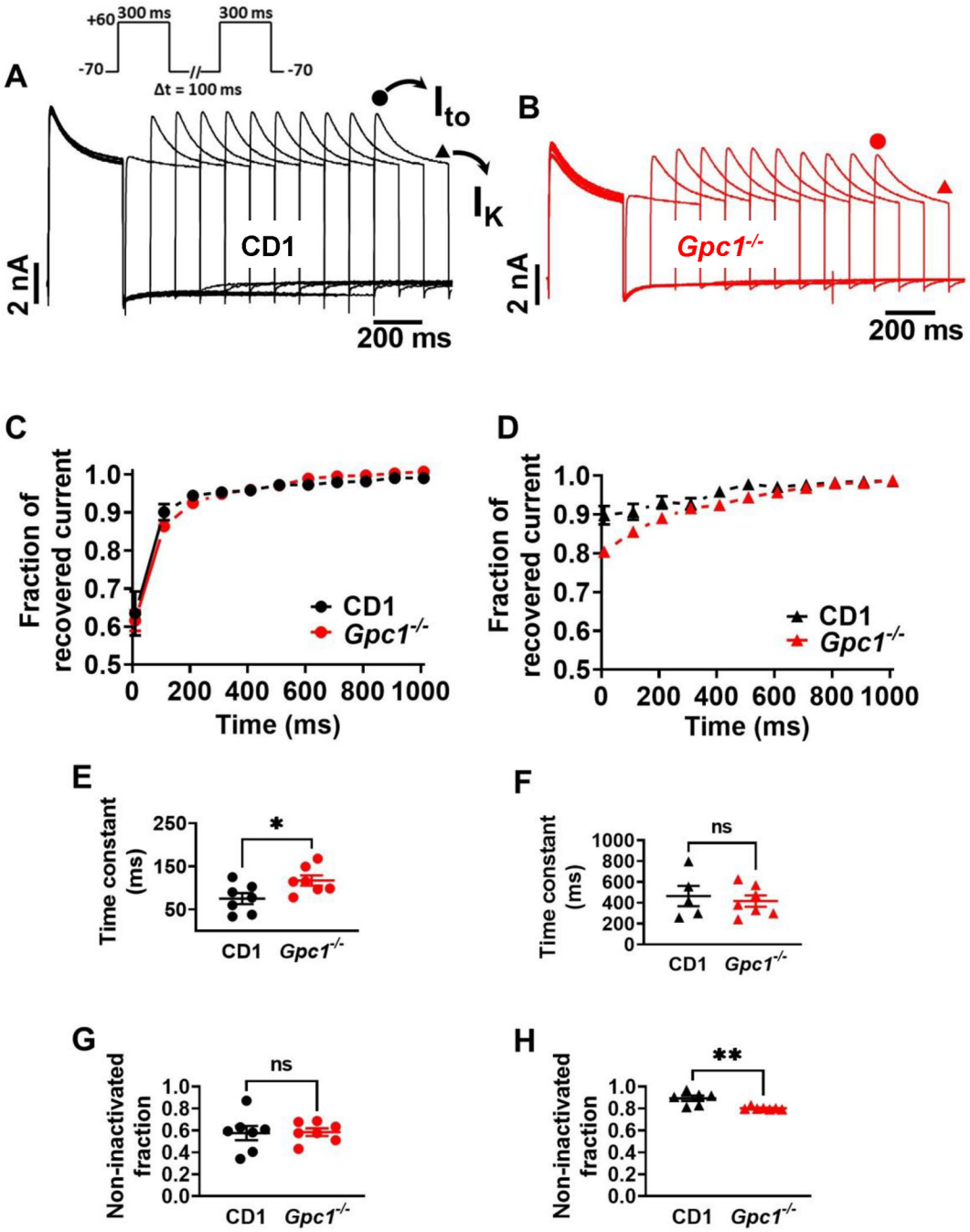

Figure 5. Recovery from inactivation of I_{to} and I_K in ventricular myocytes from CD1 and *Gpc1*$^{-/-}$ mice.

A and **B**, typical current traces recorded in voltage-clamped (protocol in the inset) for the study of the recovery from inactivation of I_{to} and I_K in ventricular cardiomyocytes from CD1 (**A**, black) and *Gpc1*$^{-/-}$ (**B**, red) mice (see methods section for details). Transient outward K^+ currents (I_{to}) were taken from the peak of the recorded currents (circles) delay rectifier K^+ currents (I_K) were taken at the end of a 300-ms depolarizing pulse (triangles) and indicated in the figure. **C** and **D**, individual current values for Ito or IK elicited by the

Health Research Alliance Author Manuscript

second depolarization to +60 mV were normalized by the values for the same type of current but during the first depolarization to +60 mV. Normalized values were averaged and plotted against the time to recover period at −70 mV for I_{to} (**C**) and I_K (**D**). Note that the recovery from inactivation of I_K is remarkably different between datasets from CD1 and *Gpc1*$^{-/-}$ mice showed in **D**. The individual recovery from inactivation plots (one per cell) were fitted with a single exponential to generate a time constant and a non-inactivated fractional value that is the level of current after a 10-ms time at −70 mV (the shortest of the series). **E** and **F**, For I_{to} recovery from inactivation, but not I_K, the time constant of the data from *Gpc1*$^{-/-}$ was statistically different from CD1 data. **G** and **H**, however, the non-inactivated fraction was remarkably different on for IK. More analysis details and parameters are showed in Table 6. All plotted data are presented as means ± S.E.M. (n = 8–10). * Denotes P<0.05 and ** denotes P<0.01 when tested with unpaired Student's t-test.

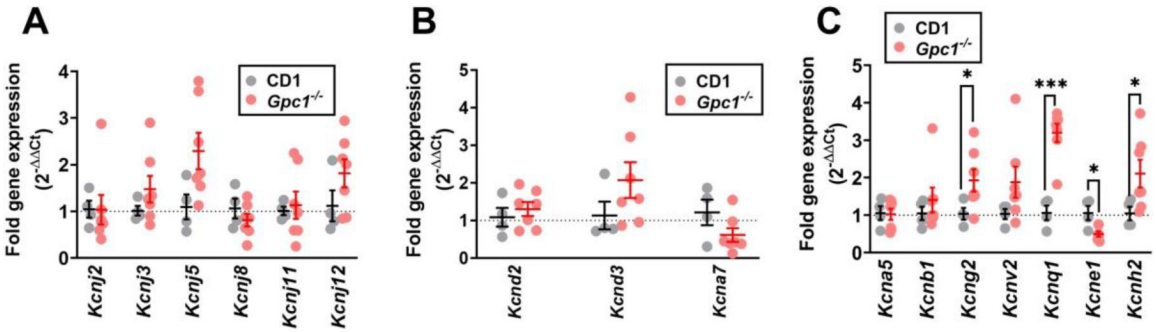

Figure 6. mRNA transcription of K^+ channels genes in ventricular cardiac tissue from CD1 mice and *Gpc1*$^{-/-}$ mice.

Relative expression of K^+ channels subunits related to I_{K1} currents (**A**), I_{to} (**B**) and I_K (**C**). Data from CD1 (gray circles for individual data and black lines for mean ± S.E.M, n=5) and from *Gpc1*$^{-/-}$ (light red circles for individual data and red lines for mean ± S.E.M, n=9) are represented as relative gene expression ($2^{-\Delta\Delta}$Ct), using *Eef1e1* as the housekeeping gene [14]. * Denotes $P < 0.05$ and *** denotes $P<0.001$ from unpaired two-tailed Student's t-test.

Table 1.

Echocardiographic parameters from CD1 and *Gpc1*$^{-/-}$ mice.

	CD1	*Gpc1*$^{-/-}$
End-systolic volume (μL)	37.24 ± 3.16 (n=10)	35.87 ± 2.12 (n=10)
End-diastolic volume (μL)	83.65 ± 4.36 (n=10)	88.75 ± 3.48 (n=10)
Ejection Fraction (%)	55.92 ± 1.97 (n=10)	59.78 ± 1.46 (n=10)
Stroke volume (μL)	46.42 ± 2.02 (n=10)	52.89 ± 2.07 (n=10) *
Cardiac Output (mL/min)	20.55 ± 1.04 (n=10)	26.28 ± 1.45 (n=10) *

Data are represented as means ± S.E.M. The number of independent experiments (mice) are indicated between parentheses).

* Denotes $p<0.05$ when comparing CD1 vs *Gpc1*$^{-/-}$ with unpaired Student's t-test.

Table 2.

Electrocardiographic parameters from CD1 and *Gpc1*$^{-/-}$ mice.

	CD1	*Gpc1*$^{-/-}$
Heart rate (bpm)	514.3 ± 38.86 (n=6)	569.8 ± 20.79 (n=6)
PR interval (ms)	40.33 ± 1.33 (n=6)	41.33 ± 2.26 (n=6)
QRS complex (ms)	11.17 ± 0.54 (n=6)	11.33 ± 0.71 (n=6)
QT interval (ms)	29.50 ±0.95 (n=6)	36.17 ± 2.04 (n=6)
QTc interval (ms)	85.76 ± 3.11 (n=6)	111.3 ± 6.48 (n=6) *
T wave duration (ms)	18.67 ± 1.43 (n=6)	24.33 ± 2.07 (n=6) *
Abnormal ST segments (%) #	0 (n=6)	67 ǂ (n=6) ǂ

Data presented as mean ± SEM, except for the abnormal ST segments analysis. The number of independent experiments (mice) are indicated between parenthesis.

# indicates one hundred P-QRS-T complexes per animal were analyzed.

ǂ denotes $p<0.05$ with Fisher's exact test.

* Denotes $p<0.05$ when comparing CD1 vs *Gpc1*$^{-/-}$ with unpaired Student's t-test.

Health Research Alliance Author Manuscript

Table 3.

Resting potential values and action potentials' parameters in ventricular cardiomyocytes from CD1 and *Gpc1*$^{-/-}$ mice.

	CD1	*Gpc1*$^{-/-}$
Resting potential (mV)	−89.94 ± 2.34 (n=10)	−86.05 ± 1.91 (n=11)
Action potential peak (mV)	18.80 ± 4.32 (n=11)	23.48 ± 3.46 (n=11)
Action potential amplitude (mV)	108.70 ± 4.06 (n=11)	109.50 ± 2.53 (n=11)
Maximal dV_m/dt (mV/ms)	139.70 ± 8.92 (n=11)	114.90 ± 8.67 (n=11)
Minimal dV_m/dt (mV/ms)	−18.66 ± 1.26 (n=11)	−19.10 ± 1.83 (n=11)

Data presented as mean ± SEM. All datasets were submitted to unpaired Student's t-test, resulting in no differences between CD1 and *Gpc1*$^{-/-}$ related data. The number of independent experiments (n) is shown between parentheses.

Table 4.

K^+ conductance activation voltage-dependent parameters.

		CD1	*Gpc1*$^{-/-}$
I_{to}	**V_{50} (mV)**	−16.22 ± 1.81 (n=9)	−11.05 ± 1.99 (n=8)
	Slope (mV/e-fold)	14.23 ± 1.30 (n=9)	15.06 ± 1.48 (n=8)
I_K	**V_{50} (mV)**	−3.55 ± 2.61 (n=9)	15.08 ± 3.69 (n=8) ***
	Slope (mV/e-fold)	17.32 ±3.14 (n=9)	15.98 ± 0.97 (n=8)

Data presented as mean ± SEM. The number of independent experiments (n) are indicated between parentheses.

*** Denotes p<0.001 when comparing CD1 vs *Gpc1*$^{-/-}$ with unpaired Student's t-test.

Table 5.

K^+ currents inactivation voltage-dependent parameters.

		CD1	*Gpc1*$^{-/-}$
I_{to}	**V_{50} (mV)**	−49.38 ± 1.72 (n=10)	−54.72 ± 5.90 (n=8)
	Slope (mV/e-fold)	10.99 ± 0.68 (n=10)	11.53 ± 2.03 (n=8)
	Non-inactivated fraction	0.37 ± 0.03 (n=10)	0.42 ± 0.04 (n=8)
I_K	**V_{50} (mV)**	−29.19 ± 1.66 (n=10)	−46.84 ± 6.78 (n=8) **
	Slope (mV/e-fold)	11.01 ± 2.21 (n=10)	15.31 ± 3.47 (n=8)
	Non-inactivated fraction	0.66 ± 0.04 (n=10)	0.57 ± 0.04 (n=8)

Data presented as mean ± SEM, except for the abnormal ST segments analysis. The number of independent experiments is indicated between parentheses.

** Denotes $p<0.01$ when comparing CD1 vs *Gpc1*$^{-/-}$ with unpaired Student's t-test.

Table 6.

K^+ currents recovery from inactivation parameters.

		CD1	*Gpc1*$^{-/-}$
I_{to}	**Non-inactivated fraction**	0.57 ± 0.06 (n=6)	0.58 ± 0.03 (n=6)
	Recovering time constant (ms)	75.03 ± 12.75 (n=6)	117.02 ± 11.86 (n=6) *
	Recovered fraction	0.97 ± 0.01 (n=6)	0.99 ± 0.01 (n=6)
I_K	**Non-inactivated fraction**	0.89 ± 0.02 (n=6)	0.80 ± 0.01 (n=6)**
	Recovering time constant (ms)	464.00 ± 97.95 (n=6)	415.88 ± 54.30 (n=6)
	Recovered fraction	1.01 ± 0.01 (n=6)	1.01 ± 0.01 (n=6)

Data presented as mean ± SEM, except for the abnormal ST segments analysis. The number of independent experiments (n) are indicated between parentheses.

* Denotes $p<0.05$ when comparing CD1 *vs Gpc1*$^{-/-}$ with unpaired two-tailed Student's t-test.